



Meltwater of freeze-thaw cycles drives N₂O-governing microbial communities in a drained peatland forest soil

Fahad Ali Kazmi¹ · Mikk Espenberg¹ · Jaan Pärn¹ · Mohit Masta¹ · Reti Ranniku¹ · Sandeep Thayamkottu¹ · Ülo Mander¹

Received: 2 April 2023 / Revised: 12 December 2023 / Accepted: 18 December 2023 / Published online: 28 December 2023
© The Author(s), under exclusive licence to Springer-Verlag GmbH Germany, part of Springer Nature 2023

Abstract

Soil freeze-thaw cycles affect N₂O fluxes in high- and mid-latitude regions, but understanding microbial processes behind N₂O will help clarify the long-term impact of freeze-thaw on climate change. The aim of this study was to investigate the impacts of freeze-thaw cycles on microbial abundances and N₂O emissions in a hemi-boreal drained peatland forest. The soil freeze-thaw experiment involved artificial heating to thaw the topsoil after freezing. Results showed that thawing of the 5 cm topsoil increased soil water content (SWC) and N₂O emissions. Microbial analysis demonstrated that the abundance of soil prokaryotes increased with thawing. N₂O emissions were negatively correlated with NH₄⁺-N while ammonia-oxidizing archaea and bacteria, including complete ammonia oxidizers, increased their abundance. This indicates a potential nitrification pathway. The abundance of nitrite reductase genes (*nirK* and *nirS*) showed a positive correlation with N₂O fluxes, while *nosZ* genes did not increase. The results provide an insight into the impact of soil freeze-thaw cycles on N₂O fluxes and the underlying microbial processes. The dynamics of SWC during the thawing period were the most direct driver of the increase in N₂O emissions. Incomplete denitrification was the dominant process for the N₂O emissions during the thaw. More than 80% of produced N₂O was denitrified to inert N₂, as shown by high potential N₂ emissions. The frequency of freeze-thaw events is expected to increase due to climate change; therefore, determining the underlying microbial processes of the N₂O emissions under freeze-thaw is of great importance in predicting possible impacts of climate change in forests.

Keywords Soil water content · Nitrification · Denitrification · Greenhouse gases · Climate change

Introduction

Nitrous oxide (N₂O) is a strong greenhouse gas and a major depleter of the stratospheric ozone layer (Ravishankara et al. 2009). N₂O is mainly produced in the soil through the oxidation of ammonia by nitrifiers (*amoA*-carrying microbes) and the reduction of nitrates by denitrifiers (usually described by *nirS* and *nirK* genes possessing microbes). During denitrification, N₂O can be released if the denitrifiers possessing *nosZI* and *nosZII* genes consume less N₂O than is produced (Firestone et al. 1980; Braker and Conrad 2011; Graf et al. 2014). Long-term monitoring has shown that one of the hot moments of N₂O

emissions is the freeze-thaw phenomenon (Mander et al. 2021). Seasonal soil freezing and thawing affect 55% of the Northern Hemisphere, especially mid to high-latitudes and high-elevation areas (Phillips et al. 2003; Kreyling et al. 2008). Temperate mineral forest soils (Groffman et al. 2006; Goldberg et al. 2010; Peng et al. 2019), temperate and boreal peatland forest soils (Cui et al. 2016; Viru et al. 2020; Mander et al. 2021), temperate grasslands (Wu et al. 2020b), and northern agricultural soils (Wagner-Riddle et al. 2017; Pelster et al. 2019; Ejack and Whalen 2021) have shown a spike in N₂O emissions during the spring freeze-thaw period. Considering the spatial scale of the freeze-thaw phenomenon, such emissions can significantly affect the annual global N₂O emissions (Yao et al. 2010; Németh et al. 2014). Freeze-thaw events will be more frequent and extend beyond spring and autumn in the future due to climate change (Henry 2008). This will additionally affect the global N₂O budgets. Thus, a better understanding of the microbial dynamics during

✉ Fahad Ali Kazmi
fahad.ali.kazmi@ut.ee

¹ Department of Geography, Institute of Ecology and Earth Sciences, University of Tartu, Vanemuise Street 46, 51003 Tartu, Estonia

freeze-thaw events can help advance the knowledge necessary for understanding N_2O emission processes.

The precise underlying mechanism driving the N_2O emissions during freeze-thaw events is not fully explained yet, and a generally accepted theory is lacking. Teepe et al. (2001) found that the frozen soil layer may trap the N_2O produced underneath, and the gas is released as the top layer thaws. However, Wang et al. (2008) argue that in such cases, trapped N_2O should be converted into N_2 through denitrification unless the temperature below the surface also gets too low for N_2O reducers. Risk et al. (2013) found these emissions to be *de novo* and the result of microbial activity. The availability of substrate and microbial activity are among the main players behind N_2O emissions at low temperatures (Öquist et al. 2004; Sharma et al. 2006; Wang et al. 2008; Peng et al. 2019). A freezing period is followed by the increased availability of substrates (ammonia, nitrate, dissolved organic N) in the soil (Matzner and Borken 2008; Song et al. 2017), which are then consumed upon thawing by microbes in the presence of higher soil moisture (Chen et al. 2015). Many studies on freeze-thaw fluxes have found denitrification to be the dominant process behind N_2O emissions (Müller et al. 2002; Öquist et al. 2004; Ludwig et al. 2004; Koponen et al. 2006; Mørkved et al. 2006; Risk et al. 2013). Especially in this regard, Holtan-Hartwig et al. (2002) found that N_2O -reducing microbial communities (denitrifiers possessing *nosZI* and *nosZII* genes) show a breakdown in their growth at a temperature below 5 °C. However, the N_2 fluxes during the freeze-thaw cycles, which could give further insight into N_2O production and reduction processes, have only been examined by a few previous studies (Wu et al. 2020a), and no work has been done on peat soils.

Boreal and sub-arctic regions comprise 87% of worldwide peatlands (Vitt 2006). Out of those (34.6 Mha), nearly half (15 Mha) have been drained for forestry (Paavilainen and Päivänen 1995). Drained boreal peatlands, often rich in nutrients, are exposed to the seasonal freeze-thaw phenomenon and can substantially contribute to annual N_2O emissions. During the freeze-thaw period, the N_2O emissions from peatlands are 8–10 times higher than average N_2O emissions (Mander et al. 2021) and are mainly related to surface temperature, soil moisture, and availability of nitrate and ammonium (Cui et al. 2016; Song et al. 2022). However, the microbial dynamics in peatlands during the freeze-thaw period have not been extensively studied.

This study aims to understand the N_2O emission process in hemi boreal peatlands during the freeze-thaw period using the abundance of functional genes involved in the N-cycle. Our hypotheses are as follows: during the freeze-thaw period, (1) soil surface temperature and soil water content (SWC) have a significant impact on N_2O flux, (2) ammonia oxidizers, including newly discovered complete ammonia

oxidizers (COMAMMOX), influence N_2O emissions, and (3) denitrifiers are leading the N_2O emissions.

Methodology

Experimental set-up

A drained peatland mixed forest, dominated by Norway spruce (*Picea abies*) and Downy birch (*Betula pubescens*), near the Agali Village of Kastre Municipality, Southeast Estonia, was the study site (58.290184, 27.31725) for the experiment conducted in March 2022 (Fig. 1). The average day-time air temperature in March is 2 °C, falling to −5 °C at night, making March a suitable time of the year to study *in situ* freezing and thawing processes. A total of fifteen collars with a diameter of 50 cm were installed for N_2O emission measurements — twelve on the ground and three on the snow. Heating cables (50W) were laid on the ground surface inside nine collars. The remaining six collars were considered control groups, three without snow, and three covered with snow.

The experimental thawing and freezing were repeated on the 7th, 13th, and 23rd of March 2022, and the sites were sampled at three moments: before heating (S1), after 2 h of heating (S2), and after 4 h of heating (S3). Control measurements were taken once per day from the unheated and snow-covered. The heating stayed on during sampling time and was turned off after the S3 to ensure freezing of the topsoil during the night.

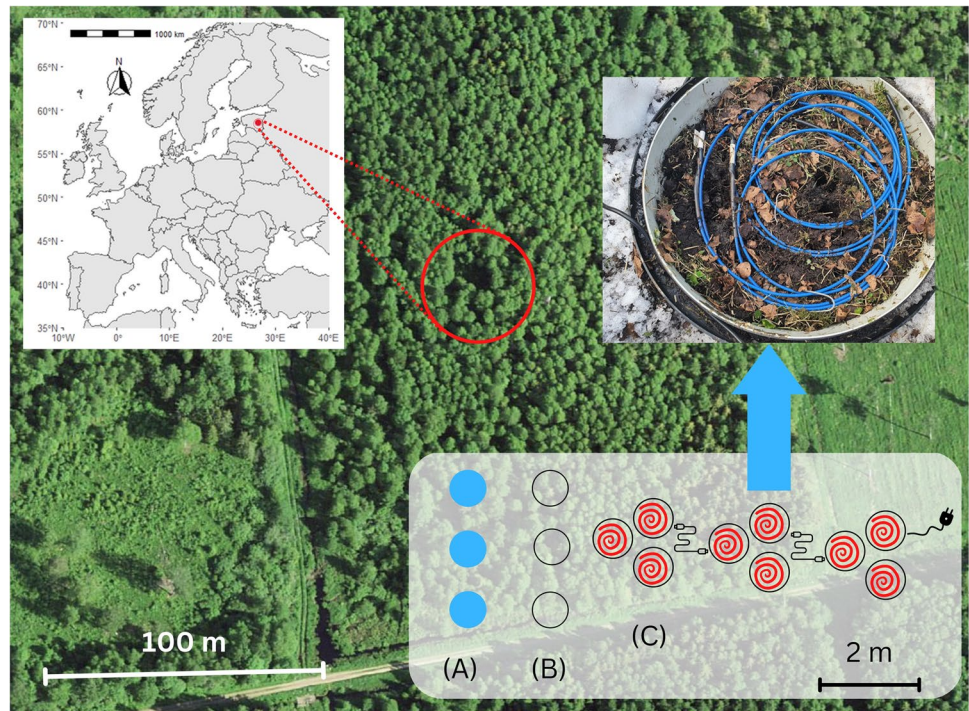
Soil sampling, physical, and chemical analyses

Three soil sampling campaigns were made on the 7th, 13th, and 23rd of March 2022. In every sampling session, 100–200 g soil samples from a maximum depth of 10 cm were collected. Soil samples for chemical analysis were stored at 4 °C, whereas the samples for microbiological analysis were stored at −20 °C. During each sampling session, the temperature on the soil surface was recorded using a temperature probe (model CS 107, Campbell Scientific Inc., Logan, UT, USA). Soil moisture was measured using the ProCheck moisture sensor (Decagon Devices, Inc., USA). The soil chemical analyses were carried out at the Estonian Environmental Research Centre in Tartu. Flow-injection analysis (APHA-AWWA-WEF, 2005) was performed to determine ammonium (NH_4^+ -N) and nitrate (NO_3^- -N) from a 2M KCl extract (1:10 ratio) of the soil samples.

N_2O sampling

Gas samples were collected from 65 L polyvinyl chloride chambers put on pre-installed collars and injected into 50

Fig. 1 Experimental scheme of sampling spots with different treatment conditions: control collars covered with snow (A), control collars with no treatment (B), and experimental collars equipped with heating cables (C). The experimental setup was installed in Estonia's drained peatland forest dominated by Norway spruce (*Picea abies*) and Downy birch (*Betula pubescens*)



mL pre-vacuumed glass bottles (Soosaar et al. 2011) before heating (S1), after the first heating session (S2) and after the prolonged heating session (S3). Every gas sampling session lasted 1 h, with sample collection at 0, 20, 40, and 60 min. All gas samples were tested for N_2O concentration using two Shimadzu-2014 gas chromatographs equipped with an electron capture detector (GC-ECD), a thermal conductivity detector (GC-TCD), and a Lofthfield-type autosampler. Fluxes were calculated from the slope of the least-squares linear regression of the change of N_2O concentrations in the chamber headspace over the measurement time.

N_2 sampling and analysis

The helium atmosphere (He-O) soil incubation method was used to measure potential N_2 fluxes from soil cores ex situ (Butterbach-Bahl et al. 2002; Mander et al. 2014). On each measurement day, intact soil cores (diameter 6.8 cm, height 6 cm) were collected from the topsoil (0–10 cm) of control plots with (total $n = 9$) and without snow ($n = 9$) and from heating plots ($n = 18$) after the gas sampling at S3. The cylinders were kept at ambient soil temperature at collection time and transported to the University of Tartu laboratory to be placed into gas-tight incubation vessels located in a climate chamber at field temperature (0.5 °C). Ambient gases were removed from incubation vessels by flushing with an artificial gas mixture (21.0% O_2 , 358 ppm CO_2 , 0.313 ppm N_2O , 1.67 ppm CH_4 , 5.97 ppm N_2 , and He). The new atmosphere equilibrium was established after 12–24 h of continuous flushing of the vessel headspace with the artificial gas

mixture at 20 mL/min. N_2 fluxes were determined using the gas chromatograph (Shimadzu GC-2014) equipped with a thermal conductivity detector, detecting N_2 concentration changes in the mixture of emitted gases accumulated in the vessel headspace of the cylinder after 2 h of closure (concentrations measured at 0, 40, 80, and 120 min). Fluxes were calculated applying linear regression, and flux measurements with R^2 of 0.81 or greater ($p < 0.1$) were used.

DNA extraction

From 0.25 g of the collected soil, DNA was extracted using the DNeasy PowerSoil Pro kit (Qiagen, Hilden, Germany) according to the manufacturer's protocol provided with the kit. Before DNA extraction, the soil was homogenized with lysis buffer using Precellys 24 Homogenizer (Berlin Technologies, Montigny-le-Bretonneux, France) at 5000 rpm for 20 s. An Infinite M200 spectrophotometer (Tecan AG, Grodig, Austria) was used to determine the extracted DNA's concentration and quality before it was stored at -20 °C.

Quantitative polymerase chain reaction (qPCR)

Using RotorGene® Q equipment (Qiagen, Valencia, CA, USA), the qPCR assays of 16S rRNA genes were performed to determine the abundance of the bacterial and archaeal communities. To determine nitrifier abundance, we quantified bacterial *amoA* (ammonia monooxygenase gene), archaeal *amoA*, and COMAMMOX (complete ammonia oxidation) *amoA* genes by qPCR. Similarly, denitrification

genes *nirK* (copper-containing nitrite reductase gene), *nirS* (cytochrome cd1-type nitrite reductase gene), *nosZI* (clade I nitrous oxide reductase gene), and *nosZII* (clade II nitrous oxide reductase gene) were quantified with qPCR. The data obtained from qPCR was analyzed using RotorGene Series Software (version 2.0.2, Qiagen, Hilden, Germany) and LinRegPCR program v. 2020.0. The abundance of different genes was expressed as copies per gram of dry soil (gene copies g^{-1} dw). Primer concentrations and the qPCR method were chosen according to Espenberg et al. (2018). The DNA extraction and qPCR were carried out in the microbiology lab of the Department of Geography at the University of Tartu.

Statistical analyses

Minitab® (v21.1.1) was used for the descriptive analyses (means, medians, and variances). RStudio (R version 4.2.0) was used to assess the normality of the data by performing Shapiro-Wilk tests and creating quantile-quantile (Q-Q) plots, and histograms for each session. In RStudio, the *ggstatsplot* package was used to perform Welch's ANOVA to compare the means across the sessions. To account for the violation of variance homogeneity, robust statistical methods were employed for further analysis. Games-Howell tests were conducted as post hoc comparisons to identify any

significant pairwise differences. The \log_{10} values of the gene copy number (g^{-1} , dw) were calculated and used in a principal component analysis (PCA). The proportions of genes in the total microbial abundance were calculated directly from the gene copy numbers, and an arcsine transformation was applied to the proportions before further analyses. PCA plots were created using the *ggbiplot* package, while other figures were created using the *ggplot2* package in RStudio. Simple linear and multiple regression models were also employed to determine correlations between different parameters. Spearman correlations were performed between SWC and temperature, and N_2O and SWC separately in controls and treatment.

Results

Soil physical and chemical parameters

In the experimental setup, the temperature in the snow-covered soil and the control chambers remained between 0 and 1 °C, while it ranged between 0 and 4 °C in the artificially heated soil (Fig. 2). SWC in snow-covered soil ranged from 0.4 to 0.6 $m^3 m^{-3}$, while in the control soil, the mean value was 0.1 $m^3 m^{-3}$ with a range from 0.1 to 0.5 $m^3 m^{-3}$. Similarly, in the soil treated with artificial heating, SWC ranged

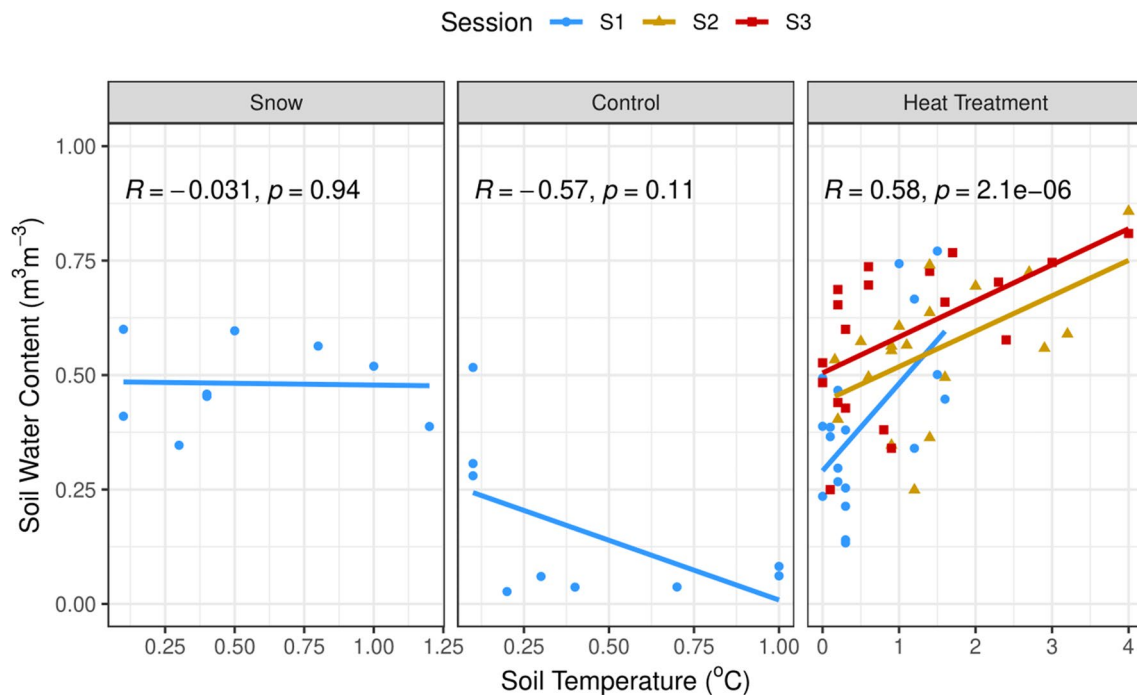


Fig. 2 Relationship between soil temperature and soil water content during the freeze-thaw experiment. Different shapes and colors represent the observations in different sessions; S1 is the session without heating, S2 is the first session with the heating on, and S3 is the ses-

sion with prolonged heating. The slopes and lines represent the best fit for the relationship between SWC and soil temperature in different sessions

between 0.1 and 0.8 m³ m⁻³, showing mean values of 0.5 and 0.6 in S2 and S3, respectively. The heating resulted in a significant change in the soil temperature ($p = 0.001$) as well as SWC ($p < 0.001$). The correlation between soil temperature and SWC was significantly positive in the heated soil (Fig. 2). The heating-induced thawing of the topsoil layer was also visible during the experiment.

NH₄⁺-N in soil decreased through the heating sessions ($p < 0.05$) from a mean value of 11.4 mg N kg⁻¹ in S1 to 7 and 6 mg N kg⁻¹ in S2 and S3, respectively, and the change was most significant between S1 and S3 ($p = 0.002$) (Fig. 3). NO₃⁻-N showed an increasing trend in response to heating, with the mean values increasing from 31 mg N kg⁻¹ in S1 to 35 and 36 mg N kg⁻¹ in S2 and S3, respectively. Only on day 1, NO₃ decreased in S3 in comparison to session S1, while on other days, it kept increasing in the heated chambers. The variation in nitrate levels, however,

was statistically insignificant ($p > 0.05$). In the soil treated with heating cables, nitrate was negatively correlated with ammonia ($p = 0.05$).

N₂O and N₂ emissions and physical and chemical properties

The mean N₂O flux from the soil before heating (S1) was 72.9 μg N m⁻² h⁻¹, increasing to 107 μg N m⁻² h⁻¹ upon heating in S2. Emissions peaked in S3 with a mean value of 128.5 μg N m⁻² h⁻¹. On day 1, the N₂O emissions increased in response to heating in S2 and showed a significant increase in S3 (Fig. 4). There was a small and statistically insignificant difference in N₂O emission between S1 and S2 on day 2. However, emissions in S3 for all days showed a statistically significant difference ($p = 0.02$) from S1 (Fig. 4).

Fig. 3 Variation in soil ammonium (NH₄⁺-N) and soil nitrate (NO₃⁻-N) against sampling sessions of the freeze-thaw experiment. S1 is the session without heating, S2 is the first session with heating on, and S3 is the session with prolonged heating. The box in the boxplot indicates the 25th and 75th percentile while whiskers show the range of all data points, excluding outliers. The intersected line in the box represents the median

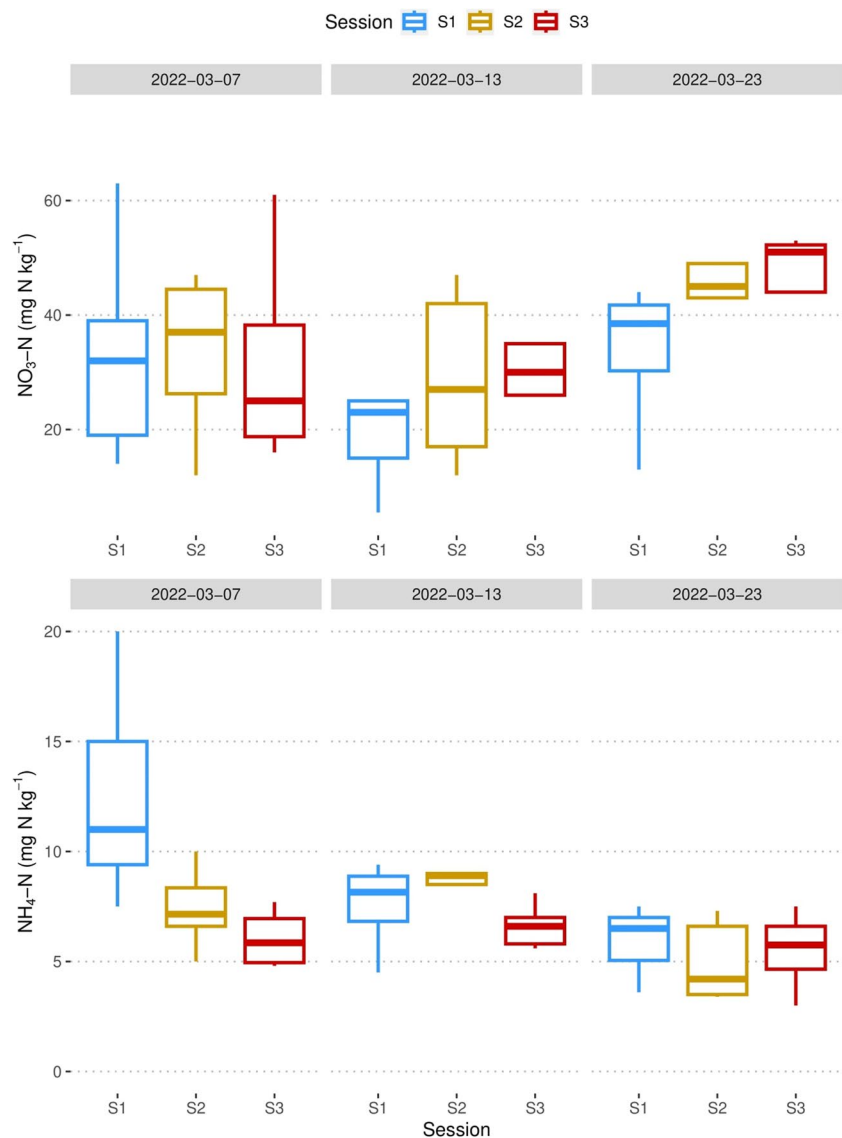
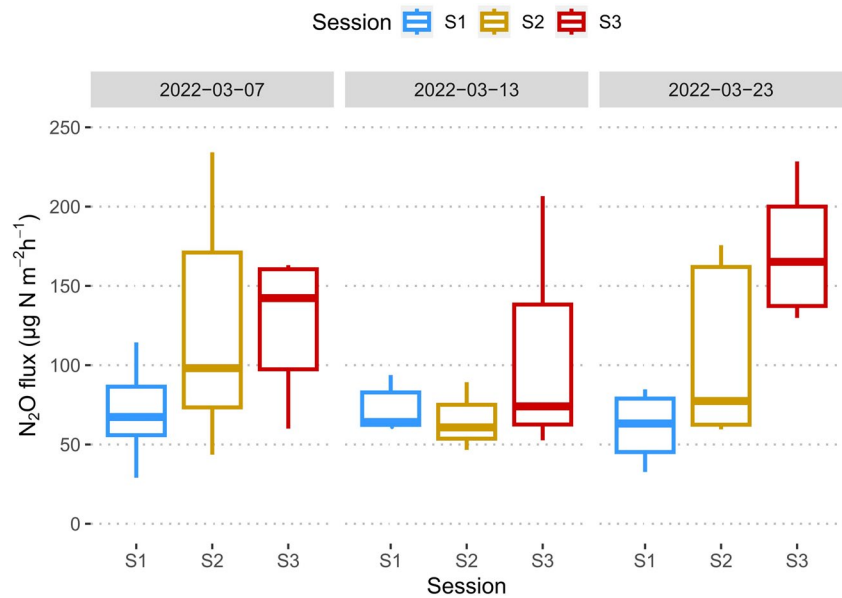


Fig. 4 The N_2O emissions based on different days for the three sampling sessions. S1 is the session without heating, S2 is the first session with heating on, and S3 is the session with prolonged heating. The mean values show a significant difference between S1 and S3 ($p < 0.05$). The box in the boxplot indicates the data points between the 25th and 75th percentile while whiskers show the range of all data points excluding the outliers. The intersected line in the box represents the median



N_2O emissions measured from incubated soil cores were $2.2 \mu\text{g N m}^{-2} \text{h}^{-1}$ on average in the control chambers without snow, $0.9 \mu\text{g N m}^{-2} \text{h}^{-1}$ in the control chambers with snow, and $10.9 \mu\text{g N m}^{-2} \text{h}^{-1}$ in the heated plots after S3 (Fig. 5A). Average N_2 emissions from the incubated soil samples were $1315.3 \mu\text{g N m}^{-2} \text{h}^{-1}$, $1293.2 \mu\text{g N m}^{-2} \text{h}^{-1}$, and $1555.4 \mu\text{g N m}^{-2} \text{h}^{-1}$ on the respective treatment plots (Fig. 5B). The emissions did not show statistically significant differences between treatments. The soil N_2O

sink capacity ratio $\text{N}_2\text{O}:(\text{N}_2\text{O}+\text{N}_2)$, indicating a potential N_2O production (N_2O) to total denitrification ($\text{N}_2\text{O} + \text{N}_2$) in soil, was on average 0.0008, 0.0006, and 0.006 in control, snow, and heating plots, respectively (Fig. 5C). There were no significant differences between the different treatments. Higher ratios indicate lower soil N_2O sink capacity, as the share of N_2O as the gaseous product of the denitrification process is higher, and therefore lower ratio values, i.e., higher soil sink capacity, show that more of

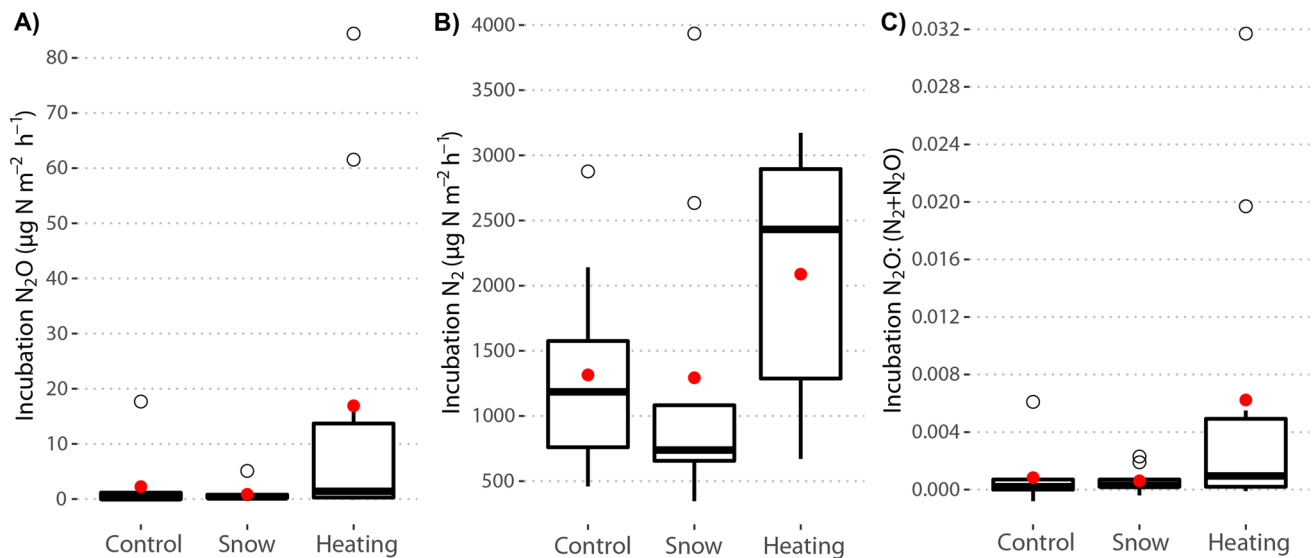


Fig. 5 Boxplots showing **A** N_2O emissions, **B** N_2 emissions, and **C** soil N_2O sink capacity, indicated by the $\text{N}_2\text{O}:(\text{N}_2+\text{N}_2\text{O})$ ratio, from the soil incubation measurements on different treatment plots (control without snow, control with snow, heating) across the three measurement days (07/03/2022, 13/03/2022, 23/03/2022). The box

boundaries indicate data points between the 25th and 75th percentile, whiskers show the range of all data points excluding the outliers, the intersected line in the box represents the median, red dots represent mean values, and black circles show outlier values

the available N_2O is further reduced to N_2 as the denitrification process is complete.

The heating induced a significant change in SWC ($p < 0.001$). The snow-covered soil showed N_2O fluxes close to zero, although the SWC values varied greatly. The soil under the control conditions showed N_2O emissions at the lowest SWC values and showed no significant variation along the SWC increase. In the heated soil, N_2O fluxes increased with SWC values. The fluxes peaked during S3 along with peak SWC (Fig. 6; positive correlation with SWC; $p = 0.005$).

Gene abundances and proportions

The qPCR results showed that mean prokaryotic abundance in snow-covered soil was 1.8×10^{11} gene copies g^{-1} dw, while in the snow-free untreated control soil it was 2×10^{11} gene copies g^{-1} dw. The abundance ranged from 2.3×10^{10} to 6.8×10^{11} gene copies g^{-1} dw in the soil treated with heating during the different sessions of the experiment. The proportion of bacteria in the total prokaryotic abundance ranged from 88 to 99%. One-way ANOVA revealed that the total prokaryotic abundance (based on archaeal and bacterial 16S rRNA genes) significantly increased in response to heating ($p = 0.05$).

Bacterial *amoA* gene abundance ranged from 1.9×10^5 to 6.3×10^7 copies g^{-1} dw. The gene abundance significantly increased in S2 ($p < 0.05$), yet it decreased in the prolonged heating session (S3). The mean proportion of bacterial *amoA* gene to bacterial 16S rRNA gene abundance constituted 0.007% in S1, which upon heating increased to 0.009% in S2 yet decreased to 0.004% in S3. Archaeal *amoA* gene ranged from 1.9×10^6 to 1.2×10^9 copies g^{-1} dw, showed increased abundance after heating, and peaked in S3 ($p < 0.001$). Before heating, archaeal *amoA* genes constituted 4.6% of archaeal 16S rRNA abundance, which changed to 4% in S2 and to 5% in S3. COMAMMOX *amoA* gene abundance ranged from 5.2×10^5 to 2.6×10^8 copies g^{-1} dw. The gene abundance significantly increased between S1 and S3 ($p < 0.05$). The mean proportion of COMAMMOX gene to bacterial 16S rRNA was 0.01% in S1, which stayed the same in S2 yet changed to 0.02% in S3.

The *nirS* gene abundance ranged from 7.3×10^7 to 4.4×10^9 gene copies g^{-1} dw. The increase of *nirS* gene abundance was significant between S1 and S3 ($p = 0.005$). The proportion of *nirS* in the total prokaryotic abundance was 0.5% before heating, which stayed similar in S2 but increased to 0.8% in S3. The *nirK* gene abundance ranged from 2.5×10^8 to 2.3×10^{11} gene copies g^{-1} dw. The

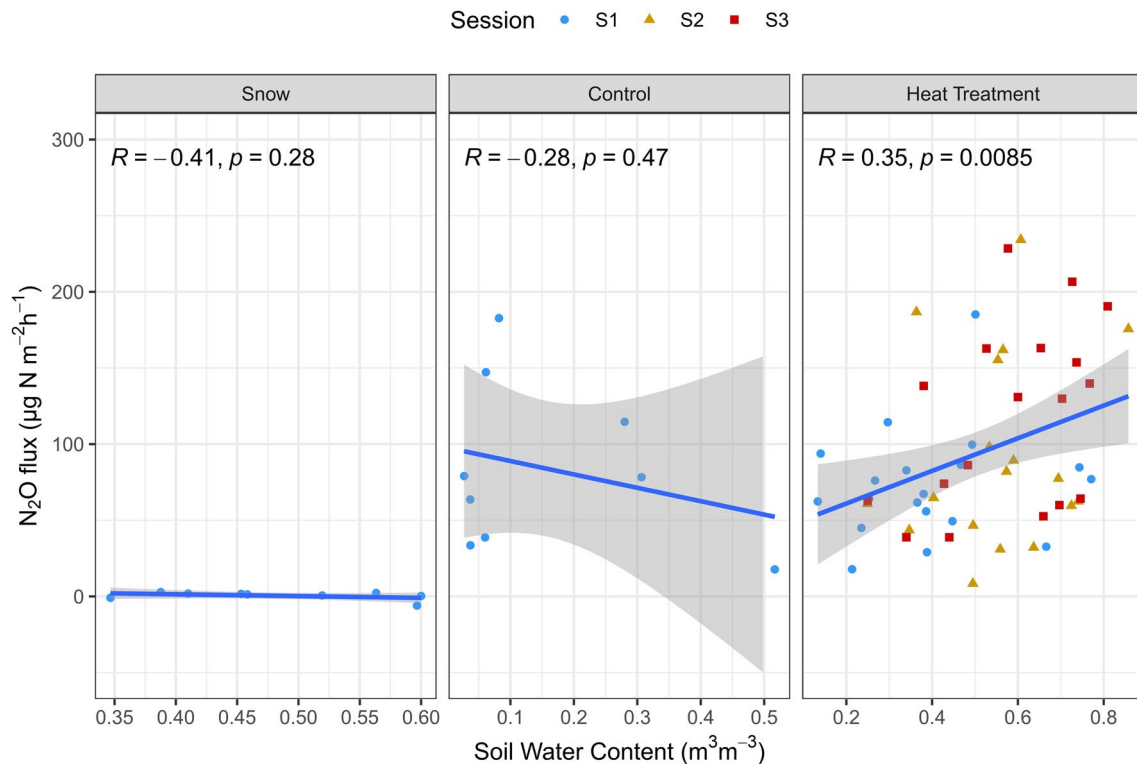


Fig. 6 Correlation between soil water content (SWC) and the N_2O fluxes in the snow-covered soil, control, and heated soil. Different colored markings indicate different measurement sessions in the treatment plot. S1 is the session without heating, S2 is the first session

with heating on, and S3 is the session with prolonged heating. The slope and line represent the best fit for the relationship between SWC and N_2O fluxes, while the grey shade represents the confidence intervals

abundance significantly increased in every heating session and peaked in S3 ($p < 0.002$). Proportion-wise, *nirK* constituted 5% of the total prokaryotic abundance in S1 and increased to 10% in S2, while it dominated in S3 with 17%.

The abundance of *nosZI* genes ranged from 1.3×10^7 to 5.1×10^9 gene copies g^{-1} dw. The abundance did not show any significant increase during the heating sessions. The mean proportion of *nosZI* genes to prokaryotic abundance remained 0.47% in S1 and S2 and dropped to 0.29% in S3. The *nosZII* gene abundance ranged from 2.9×10^7 to 7×10^9 gene copies g^{-1} dw. The abundance exhibited no significant increasing pattern throughout the two heating sessions. However, the proportion of *nosZII* genes in the total prokaryotic abundance decreased from 0.44% in S1 to 0.35% and 0.28% in S2 and S3, respectively.

The principal component analysis of the functional gene abundances (Fig. 7) showed that the functional genes dominated during both the S2 and S3 heating sessions. The functional gene abundances behaved independently but the genes encoding nitrite reductase (*nirK* and *nirS*) dominated the S3 during all days.

Relationship between gene abundances and N₂O emissions

Multiple regression models between N₂O emissions and the functional genes' abundance, as well as proportions, showed a significant positive correlation with the N₂O emissions only for *nirK* ($p < 0.05$) (Fig. 8A). The ratio of *nir* (*nirS* and *nirK*) genes to *nosZ* (*nosZI* and *nosZII*) genes varied significantly in the heating sessions ($p < 0.001$). Furthermore,

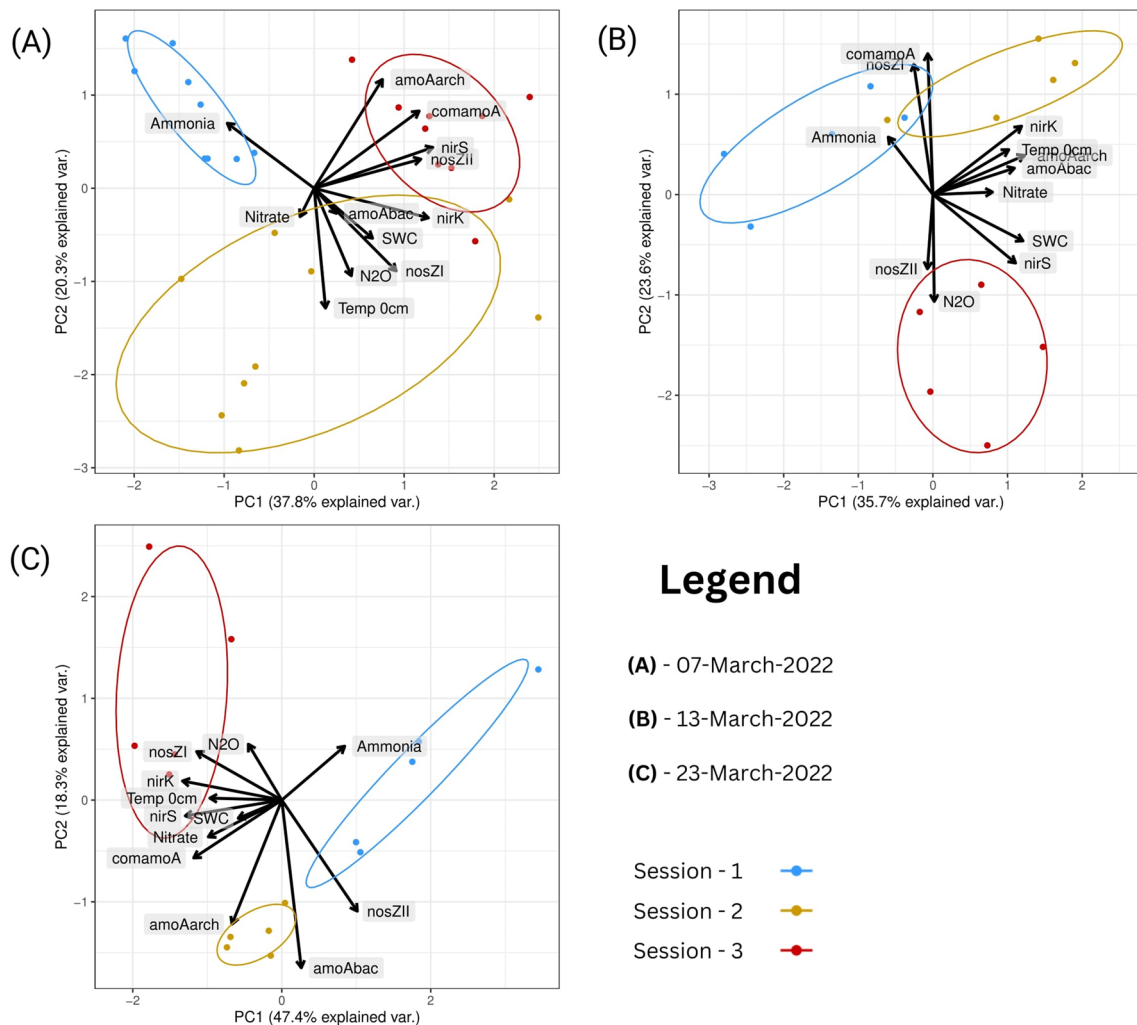


Fig. 7 Principal component analysis of the physical-chemical properties along with functional genes' abundance on 07.03.22 (A), 13.03.22 (B), and 23.03.22 (C). S1 was the session without heating, S2 was the first session with heating on, and S3 was the session with

prolonged heating. Abbreviations: amoAbac, bacterial *amoA*; amoAarch, archaeal *amoA*; comamoA, COMAMMOX *amoA*; SWC, soil water content

Fig. 8 Comparisons between gene parameters and N₂O emissions. **A** Regression coefficients; multiple regression models of N₂O emissions with abundance and proportions of different functional genes. **B** Linear regression between the ratio of *nir* genes (*nirK* and *nirS*) to *amoA* genes (bacterial *amoA* and archaeal *amoA*). **C** Linear regression between the N₂O emissions and the ratio of *nir* genes to *nosZ* genes (*nosZI* and *nosZII*)

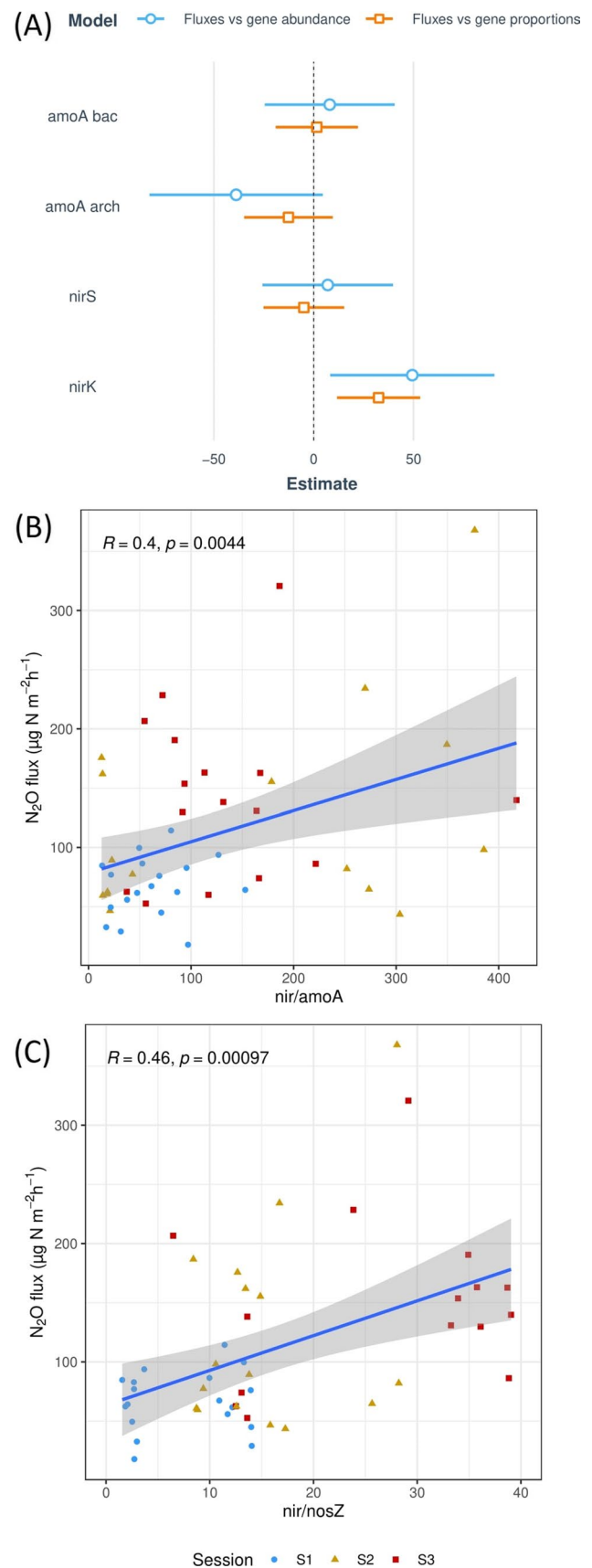
positive correlations ($p < 0.01$) were observed between N₂O emissions and the ratio of N₂O producers to reducers (*nir/nosZ*) as well as the ratio of denitrification genes to nitrification genes (*nir/amoA*) (Fig. 8B and C).

Discussion

This study aimed to elucidate N₂O emission processes during freeze-thaw events in a drained peatland forest under changing temperatures and soil water regimes by providing insights into microbial dynamics. By increasing our understanding of this phenomenon in the N-rich soil of peatlands, we aim to enrich the knowledge regarding N₂O emissions. This knowledge will help predict and model future trends of N₂O emissions in the context of climate change.

During the experiment, the increase in the soil surface temperature due to artificial heating led to the thawing of the top-frozen peat layer. The temperature increase did not stay consistent, yet thawing conditions were achieved. Thawing increased SWC (Fig. 2), gradually affecting the availability of oxygen in the soil and influencing the dominance of the underlying microbial process. Nitrification and denitrification depend contrastingly on soil oxygen, with nitrification preferring oxic conditions and denitrification occurring under anoxic conditions. During this study, we observed the consumption of NH₄⁺-N and an increase in NO₃⁻-N (Fig. 3). The increase in soil NO₃⁻-N content indicates that the thaw initiated nitrification. The increase in NO₃⁻-N was consistent throughout the measurement in S2 because this session provided aerobic conditions for the topsoil microbiome. This dynamic between NH₄⁺-N and NO₃⁻-N has also been observed in orchard soil at the same range of SWC by Wei et al. (2022) and in permafrost during freeze-thaw cycles by Song et al. (2022). The availability of substrate with increasing SWC provides a suitable environment for microbial activity thus increasing the N₂O emission potential of soil (Highton et al. 2023). The principal component analysis (Fig. 7) shows the positive loadings along the PC2 by NH₄⁺-N towards S1, which indicates the highest values of NH₄⁺-N before thawing. The angle between the vectors representing soil NH₄⁺-N and SWC also suggests a negative relationship between them.

The mean N₂O flux after the induced thawing was 117 $\mu\text{g N m}^{-2} \text{h}^{-1}$, which corresponds to a spring freeze-thaw-induced hot moment of N₂O emissions in the same drained



peatland forest (Ranniku et al. 2023). These results are smaller than the annual average in an adjacent forest, i.e., $225 \mu\text{g N m}^{-2} \text{h}^{-1}$ but considerably more than the average values in winter, which mainly stayed negative (Mander et al. 2021). N_2O emissions increased with increasing SWC and peaked at $0.5\text{--}0.7 \text{ m}^3 \text{ m}^{-3}$. Previous studies also reported the highest N_2O emissions in the same range of SWC (Pärn et al. 2018; Bahram et al. 2022). The peak N_2O emission values have also been observed in the same range of SWC during the thawing of frozen soil (Teepe et al. 2004; Koponen and Martikainen 2004; Singurindy et al. 2009). However, a freeze-thaw hot moment in the same forest occurred under higher average SWC values of $0.88 \text{ m}^3 \text{ m}^{-3}$ (Ranniku et al. 2023). Increasing SWC from meltwater boosts microbial activity and activates the soil N substrate (Wang et al. 2013). The thawing increased topsoil SWC and created suitable conditions for nitrification and incomplete denitrification. Previous studies observed a similar increase in N_2O emissions with rising soil moisture (van der Weerden et al. 2012; Banerjee et al. 2016; Wu et al. 2020b; King et al. 2021; Lin and Hernandez-Ramirez 2022).

Our study found a significant increase in the abundance of bacteria after thawing. The observed increase in bacterial abundance with increasing SWC resembles the behavior of bacteria in rewetted dry soils (Leizeaga et al. 2022). The bacterial nitrifiers increased their abundance with the onset of thawing. The increase in $\text{NO}_3^- \text{-N}$ in S2 shows the nitrification potential in thawing soil. Although the bacterial *amoA* abundance did not remain high in S3, the archaeal *amoA* and the COMAMMOX gene abundance kept increasing with thawing and peaked at the elevated SWC conditions. This can be attributed to the richer archaeal diversity in hemi boreal pristine environments (Aalto et al. 2018), and the resilience of ammonia-oxidizing archaea in prolonged anoxic conditions (Pett-Ridge et al. 2013). The same behavior of COMAMMOX also indicates their tolerance towards varying SWC and oxygen conditions. Even while the SWC variation in this study allowed the COMAMMOX to dominate over both the ammonia-oxidizing bacteria and archaea, a temperature $> 4 \text{ }^\circ\text{C}$ is necessary for their growth (Shi et al. 2020).

We also observed a significant increase in denitrifiers' (*nirK* and *nirS*) abundance in the thawing soil (Figs. 7 and 8A), as found by a previous study (Smith et al. 2010). The variation in all functional genes matches a previous study on spring freeze-thaw (Yin et al. 2019). However, unlike that study, we found a positive correlation between the abundance of *nir* genes and N_2O fluxes (Fig. 8B and C). Based on the co-occurrence patterns of *nirS* and *nosZ* genes in denitrifiers, it is evident that the *nirS*-containing microbes are more capable of complete denitrification. In contrast, an ecosystem dominated by *nirK*-type denitrifiers would emit more N_2O (Jones et al. 2008; Graf et al. 2014;

Espenberg et al. 2018). We found dominance of *nirK* gene abundance during our experiment, which matches previous findings (Clark et al. 2012; Thomson et al. 2012; Graf et al. 2014). Anaerobic conditions induced by the increased SWC (Shaaban et al. 2018) or flooding (Ligi et al. 2014) favor the activity of N_2O reducers and in such cases, *nosZI* plays an important role in N_2O consumption (Wang et al. 2022). We found no significant change in *nosZ* gene abundances in response to the increase in SWC during this study because thawing did not create flooded conditions. The soil surface temperature also did not exceed $4 \text{ }^\circ\text{C}$ during our experiment, and the abundance of N_2O -producing denitrifiers is unaffected by such low temperatures, but the N_2O reducers, on the other hand, have shown a decrease in their abundance at temperatures below $5 \text{ }^\circ\text{C}$, resulting in an increase in N_2O fluxes (Holtan-Hartwig et al. 2002; Wagner-Riddle et al. 2011). However, new primer sets for *nosZ*-I have been designed recently which might offer a more comprehensive assessment of denitrifier gene carriers and their ecological patterns (Zhang et al. 2021).

Thawing of topsoil removed physical barriers to air diffusion into the soil. Nitrifiers increased their abundance with a more aerobic soil after thawing. Increasing SWC, on the other hand, turned the soil anaerobic in prolonged heating sessions, resulting in a decline of bacterial nitrifiers' abundance in S3. However, the N_2O -producing denitrifiers kept increasing, and their abundance peaked in S3 with the highest SWC values and anaerobic conditions. Although thawing increased the SWC necessary for nitrification and denitrification to start, the temperature of the soil did not increase to the extent where *nosZ*-type denitrifiers could show their enhanced capacity of N_2O reduction. Most studies report that the denitrification process drives N_2O emissions from the soil during freeze-thaw (Wagner-Riddle et al. 2008; Smith et al. 2010; Wu et al. 2010), which occurs under high SWC and anaerobic conditions (Braker and Conrad 2011; Butterbach-Bahl et al. 2013). Factors that encourage incomplete denitrification and result in N_2O emissions are created by the fluctuation in SWC during thawing conditions and the too low temperature of soil for N_2O -reducing denitrifiers.

The dynamics of soil ammonium and nitrate, microbial abundance, and N_2O fluxes indicate that both nitrification and denitrification were potentially active during our experiment. The N_2O emissions and $\text{NH}_4^+ \text{-N}$ were negatively related (Fig. 7), indicating the conversion of ammonium to nitrate via nitrification, which is also supported by the increased abundance of ammonia-oxidizing archaea and COMAMMOX after thawing. This indicates that nitrification was potentially active during our experiment. Also, the increased abundance of denitrifiers after thawing and higher contribution of *nir* genes to N_2O emission (Fig. 8B) reveals that denitrification was the dominant process in N_2O production. These findings suggest *de novo* substrate production

as well as the production of N_2O in the thawed peat. The results are consistent with previous studies, which have established that the freeze-thaw N_2O fluxes during spring are rapid and emerge most probably from incomplete denitrification (Wagner-Riddle et al. 2008; Smith et al. 2010). The increased importance of N_2O as a product of denitrification was further supported by a higher $N_2O:(N_2O+N_2)$ ratio measured after the heating sessions. The brief cycles of elevated SWC and altered microbial oxygen consumption trigger N_2 and N_2O emissions (Friedl et al. 2022), and our study revealed that the small-scale change in SWC affected the microbial dynamics as well as the emission potential of thawing peat soil.

During freeze-thaw events, the diminishing of the frozen layer on the topsoil may also cause a physical release of the underlying trapped N_2O (Teepe et al. 2001; Goldberg et al. 2010; Risk et al. 2013). The release is only significant when the frozen soil is thawed for the first time after winter, while repeated cycles of freezing and thawing would minimize the chances of this type of release. A sustained low SWC can also change forest soil from an N_2O source to an N_2O sink (Goldberg and Gebauer 2009b). In such cases, the subsoil N_2O would be subsequently consumed when diffusing upward (Wang et al. 2008; Goldberg and Gebauer 2009a). Isotope-based analyses of freeze-thaw emissions have proved that the N_2O produced during the thawing process comes from denitrification (Wagner-Riddle et al. 2008). Although the role of nitrifiers' denitrification in the substantial fluxes can be considered; however, in N-rich soil, *nirK*-based denitrifiers are more likely responsible for the emission of N_2O (Thomson et al. 2012), which was also observed during this study.

Rewetting the drained peatlands can create a stable temperature regime for *nosZ*-type denitrifiers during freeze-thaw events which in turn will result in the completion of denitrification and less N_2O emissions. Increasing the water table of drained peatland forests is a promising mitigation measure due to its ability to promote complete denitrification and maintain favorable temperatures for N_2O -reducing denitrifiers in the soil microbiome horizon.

Conclusion

The dynamics of SWC during the thawing period greatly affected N_2O -governing microbial communities. The fluctuation of soil ammonia and nitrate and the rise in nitrifying microbial abundance indicate the nitrification process triggered by the rising SWC values. The increased abundance of *nirK*-type denitrifiers, while the unchanging abundance of *nosZ*-type denitrifiers showed the incompleteness of the denitrification during the thaw. Accordingly, incomplete denitrification was the dominant process behind N_2O emissions

during the topsoil thawing in the drained peatland forests. Future research should investigate the dynamics of microbial community composition and structure during freeze-thaw events and how manipulating these communities can complete the denitrification pathway to reduce N_2O emissions under varying SWC conditions or rewetting the drained peatlands. Further research on freeze-thaw events is necessary to improve our ability to predict N_2O emission trends and create reliable emission models, crucial given the projected rise in freeze-thaw events due to climate change extending beyond typical autumn and spring seasons.

Funding This research was supported by the European Research Council (ERC) under grant agreement No 101096403 (MLTOM23415R), the European Commission through the European Regional Development Fund (the Center of Excellence EcolChange, TK-131), the European Union HORIZON-CSA project No 101079192 “Living Labs for Wetland Forest Research (LiWeFor)”, and the Estonian Research Council (grants no PRG352, MOBERC20, and MOBERC44).

Declarations

Competing interests The authors declare no competing interests.

References

- Aalto SL, Saarenheimo J, Mikkonen A, Rissanen AJ, Tirola M (2018) Resistant ammonia-oxidizing archaea endure, but adapting ammonia-oxidizing bacteria thrive in boreal lake sediments receiving nutrient-rich effluents. *Environ Microbiol* 20:3616–3628. <https://doi.org/10.1111/1462-2920.14354>
- Bahram M, Espenberg M, Pärn J, Lehtovirta-Morley L, Anslan S, Kasak K, Kõljalg U, Liira J, Maddison M, Moora M, Niinemets Ü, Öpik M, Pärtel M, Soosaar K, Zobel M, Hildebrand F, Tedersoo L, Mander Ü (2022) Structure and function of the soil microbiome underlying N_2O emissions from global wetlands. *Nat Commun* 13(1):1–10. <https://doi.org/10.1038/s41467-022-29161-3>
- Banerjee S, Helgason B, Wang L, Winsley T, Ferrari BC, Siciliano SD (2016) Legacy effects of soil moisture on microbial community structure and N_2O emissions. *Soil Biol Biochem* 95:40–50. <https://doi.org/10.1016/j.soilbio.2015.12.004>
- Braker G, Conrad R (2011) Diversity, structure, and size of N_2O -producing microbial communities in soils—what matters for their functioning? *Adv Appl Microbiol* 75:33–70. <https://doi.org/10.1016/B978-0-12-387046-9.00002-5>
- Butterbach-Bahl K, Baggs EM, Dannenmann M, Kiese R, Zechmeister-Boltenstern S (2013) Nitrous oxide emissions from soils: how well do we understand the processes and their controls? *Philos Trans R Soc Lond B Biol Sci* 368. <https://doi.org/10.1098/RSTB.2013.0122>
- Butterbach-Bahl K, Willibald G, Papen H (2002) Soil core method for direct simultaneous determination of N_2 and N_2O emissions from forest soils. *Plant Soil* 240:105–116. <https://doi.org/10.1023/A:1015870518723>
- Chen H, Mothapo NV, Shi W (2015) Soil moisture and pH control relative contributions of fungi and bacteria to N_2O production. *Microb Ecol* 69:180–191. <https://doi.org/10.1007/s00248-014-0488-0>

- Clark IM, Buchkina N, Jhurrea D, Goulding KWT, Hirsch PR (2012) Impacts of nitrogen application rates on the activity and diversity of denitrifying bacteria in the Broadbalk wheat experiment. *Philos Trans R Soc Lond B Biol Sci* 367:1235–1244. <https://doi.org/10.1098/RSTB.2011.0314>
- Cui Q, Song C, Wang X, Shi F, Wang L, Guo Y (2016) Rapid N₂O fluxes at high level of nitrate nitrogen addition during freeze-thaw events in boreal peatlands of Northeast China. *Atmos Environ* 135:1–8. <https://doi.org/10.1016/J.ATMOENV.2016.03.053>
- Ejack L, Whalen JK (2021) Freeze-thaw cycles release nitrous oxide produced in frozen agricultural soils. *Biol Fertil Soils* 57:389–398. <https://doi.org/10.1007/S00374-020-01537-X>
- Espenberg M, Truu M, Mander Ü, Kasak K, Nölvak H, Ligi T, Oopkaup K, Maddison M, Truu J (2018) Differences in microbial community structure and nitrogen cycling in natural and drained tropical peatland soils. *Sci Rep* 8:1–12. <https://doi.org/10.1038/s41598-018-23032-y>
- Firestone MK, Firestone RB, Tiedje JM (1980) Nitrous oxide from soil denitrification: factors controlling its biological production. *Science* 208:749–751. <https://doi.org/10.1126/SCIENCE.208.4445.749>
- Friedl J, Deltedesco E, Keiblinger KM, Gorfer M, De Rosa D, Scheer C, Grace PR, Rowlings DW (2022) Amplitude and frequency of wetting and drying cycles drive N₂ and N₂O emissions from a subtropical pasture. *Biol Fertil Soils* 58:593–605. <https://doi.org/10.1007/S00374-022-01646-9>
- Goldberg SD, Borken W, Gebauer G (2010) N₂O emission in a Norway spruce forest due to soil frost: concentration and isotope profiles shed a new light on an old story. *Biogeochemistry* 97:21–30. <https://doi.org/10.1007/S10533-009-9294-Z>
- Goldberg SD, Gebauer G (2009a) Drought turns a Central European Norway spruce forest soil from an N₂O source to a transient N₂O sink. *Glob Chang Biol* 15:850–860. <https://doi.org/10.1111/J.1365-2486.2008.01752.X>
- Goldberg SD, Gebauer G (2009b) N₂O and NO fluxes between a Norway spruce forest soil and atmosphere as affected by prolonged summer drought. *Soil Biol Biochem* 41:1986–1995. <https://doi.org/10.1016/J.SOILBIO.2009.07.001>
- Graf DRH, Jones CM, Hallin S (2014) Inter-genomic comparisons highlight modularity of the denitrification pathway and underpin the importance of community structure for N₂O emissions. *PLoS One* 9:e114118. <https://doi.org/10.1371/JOURNAL.PONE.0114118>
- Groffman PM, Hardy JP, Discoll CT, Fahey TJ (2006) Snow depth, soil freezing, and fluxes of carbon dioxide, nitrous oxide and methane in a northern hardwood forest. *Glob Chang Biol* 12:1748–1760. <https://doi.org/10.1111/J.1365-2486.2006.01194.X>
- Henry HAL (2008) Climate change and soil freezing dynamics: historical trends and projected changes. *Clim Chang* 87:421–434. <https://doi.org/10.1007/S10584-007-9322-8>
- Highton MP, Bakken LR, Dörsch P, Tobias-Hunefeldt S, Molstad L, Morales SE (2023) Soil water extract and bacteriome determine N₂O emission potential in soils. *Biol Fertil Soils* 59:217–232. <https://doi.org/10.1007/S00374-022-01690-5>
- Holtan-Hartwig L, Dörsch P, Bakken LR (2002) Low temperature control of soil denitrifying communities: kinetics of N₂O production and reduction. *Soil Biol Biochem* 34:1797–1806. [https://doi.org/10.1016/S0038-0717\(02\)00169-4](https://doi.org/10.1016/S0038-0717(02)00169-4)
- Jones CM, Stres B, Rosenquist M, Hallin S (2008) Phylogenetic analysis of nitrite, nitric oxide, and nitrous oxide respiratory enzymes reveal a complex evolutionary history for denitrification. *Mol Biol Evol* 25:1955–1966. <https://doi.org/10.1093/MOLBEV/MSN146>
- King AE, Rezanezhad F, Wagner-Riddle C (2021) Evidence for microbial rather than aggregate origin of substrates fueling freeze-thaw induced N₂O emissions. *Soil Biol Biochem* 160:108352. <https://doi.org/10.1016/J.SOILBIO.2021.108352>
- Koponen HT, Jaakkola T, Keinänen-Toivola MM, Kaipainen S, Tuomainen J, Servomaa K, Martikainen PJ (2006) Microbial communities, biomass, and activities in soils as affected by freeze-thaw cycles. *Soil Biol Biochem* 38:1861–1871. <https://doi.org/10.1016/J.SOILBIO.2005.12.010>
- Koponen HT, Martikainen PJ (2004) Soil water content and freezing temperature affect freeze-thaw related N₂O production in organic soil. *Nutr Cycl Agroecosyst* 69:213–219. <https://doi.org/10.1023/B:FRES.0000035172.37839.24>
- Kreyling J, Beierkuhnlein C, Pritsch K, Schloter M, Jentsch A (2008) Recurrent soil freeze-thaw cycles enhance grassland productivity. *New Phytol* 177:938–945. <https://doi.org/10.1111/J.1469-8137.2007.02309.X>
- Leizeaga A, Meisner A, Rousk J, Bååth E (2022) Repeated drying and rewetting cycles accelerate bacterial growth recovery after rewetting. *Biol Fertil Soils* 58:365–374. <https://doi.org/10.1007/S00374-022-01623-2>
- Ligi T, Truu M, Truu J, Nölvak H, Kaasik A, Mitsch WJ, Mander Ü (2014) Effects of soil chemical characteristics and water regime on denitrification genes (nirS, nirK, and nosZ) abundances in a created riverine wetland complex. *Ecol Eng* 72:47–55. <https://doi.org/10.1016/J.ECOLENG.2013.07.015>
- Lin S, Hernandez-Ramirez G (2022) Increased soil-derived N₂O production following a simulated fall-freeze-thaw cycle: effects of fall urea addition, soil moisture, and history of manure applications. *Biogeochemistry* 157:379–398. <https://doi.org/10.1007/S10533-021-00880-X>
- Ludwig B, Wolf I, Teepe R (2004) Contribution of nitrification and denitrification to the emission of N₂O in a freeze-thaw event in an agricultural soil. *J Plant Nutr Soil Sci* 167:678–684. <https://doi.org/10.1002/JPLN.200421462>
- Mander Ü, Krasnova A, Escuer-Gatius J, Espenberg M, Schindler T, Machacova K, Pärn J, Maddison M, Megonigal JP, Pihlatie M (2021) Forest canopy mitigates soil N₂O emission during hot moments. *NPJ Clim Atmos Sci* 4:1–9. <https://doi.org/10.1038/s41612-021-00194-7>
- Mander Ü, Well R, Weymann D, Soosaar K, Maddison M, Kanal A, Löhmus K, Truu J, Augustin J, Tournebize J (2014) Isotopologue ratios of N₂O and N₂ measurements underpin the importance of denitrification in differently N-loaded riparian alder forests. *Environ Sci Technol* 48:11910–11918. <https://doi.org/10.1021/ES501727H>
- Matzner E, Borken W (2008) Do freeze-thaw events enhance C and N losses from soils of different ecosystems? A review. *Eur J Soil Sci* 59:274–284. <https://doi.org/10.1111/j.1365-2389.2007.00992.x>
- Mørkved PT, Dörsch P, Henriksen TM, Bakken LR (2006) N₂O emissions and product ratios of nitrification and denitrification as affected by freezing and thawing. *Soil Biol Biochem* 38:3411–3420. <https://doi.org/10.1016/J.SOILBIO.2006.05.015>
- Müller C, Martin M, Stevens RJ, Laughlin RJ, Kammann C, Ottow JCG, Jäger HJ (2002) Processes leading to N₂O emissions in grassland soil during freezing and thawing. *Soil Biol Biochem* 34:1325–1331. [https://doi.org/10.1016/S0038-0717\(02\)00076-7](https://doi.org/10.1016/S0038-0717(02)00076-7)
- Németh DD, Wagner-Riddle C, Dunfield KE (2014) Abundance and gene expression in nitrifier and denitrifier communities associated with a field scale spring thaw N₂O flux event. *Soil Biol Biochem* 73:1–9. <https://doi.org/10.1016/j.soilbio.2014.02.007>
- Öquist MG, Nilsson M, Sörensson F, Kasimir-Klemedtsson Å, Persson T, Weslien P, Klemedtsson L (2004) Nitrous oxide production in a forest soil at low temperatures—processes and environmental controls. *FEMS Microbiol Ecol* 49:371–378. <https://doi.org/10.1016/j.femsec.2004.04.006>
- Paavilainen E, Päivänen J (1995) Peatland forestry – ecology and principles, ecological studies. Springer-Verlag, Berlin Heidelberg New York

- Pärn J, Verhoeven JTA, Butterbach-Bahl K, Dise NB, Ullah S, Aasa A, Egorov S, Espenberg M, Järveoja J, Jauhainen J, Kasak K, Klemetsson L, Kull A, Laggoun-Défarge F, Lapshina ED, Lohila A, Löhmus K, Maddison M, Mitsch WJ et al (2018) Nitrogen-rich organic soils under warm well-drained conditions are global nitrous oxide emission hotspots. *Nat Commun* 9:1–8. <https://doi.org/10.1038/s41467-018-03540-1>
- Pelster DE, Chantigny MH, Rochette P, Bertrand N, Angers DA, Zebarth BJ, Goyer C (2019) Rates and intensity of freeze–thaw cycles affect nitrous oxide and carbon dioxide emissions from agricultural soils. *Can J Soil Sci* 99:472–484. <https://doi.org/10.1139/CJSS-2019-0058>
- Peng B, Sun J, Liu J, Dai W, Sun L, Pei G, Gao D, Wang C, Jiang P, Bai E (2019) N₂O emission from a temperate forest soil during the freeze–thaw period: a mesocosm study. *Sci Total Environ* 648:350–357. <https://doi.org/10.1016/j.scitotenv.2018.08.155>
- Pett-Ridge J, Petersen DG, Nuccio E, Firestone MK (2013) Influence of oxic/anoxic fluctuations on ammonia oxidizers and nitrification potential in a wet tropical soil. *FEMS Microbiol Ecol* 85:179–194. <https://doi.org/10.1111/1574-6941.12111>
- Phillips M, Springman SM, Arenson LU (2003) Permafrost. In: Proceedings of the 8th international conference on permafrost, 21–25 July 2003. Balkema, Zurich, pp 907–912
- Ranniku R, Schindler T, Escuer-Gatius J, Mander Ü, Machacova K, Soosaar K (2023) Tree stems are a net source of CH₄ and N₂O in a hemiboreal drained peatland forest during the winter period. *Environ Res Commun* 5:051010. <https://doi.org/10.1088/2515-7620/ACD7C7>
- Ravishankara AR, Daniel JS, Portmann RW (2009) Nitrous oxide (N₂O): the dominant ozone-depleting substance emitted in the 21st century. *Science* 326:123–125. <https://doi.org/10.1126/science.1176985>
- Risk N, Snider D, Wagner-Riddle C (2013) Mechanisms leading to enhanced soil nitrous oxide fluxes induced by freeze–thaw cycles. *Can J Soil Sci* 93:401–414. <https://doi.org/10.4141/CJSS2012-071>
- Shaaban M, Wu Y, Khalid MS, Peng QA, Xu X, Wu L, Younas A, Bashir S, Mo Y, Lin S, Zafar-ul-Hye M, Abid M, Hu R (2018) Reduction in soil N₂O emissions by pH manipulation and enhanced nosZ gene transcription under different water regimes. *Environ Pollut* 235:625–631. <https://doi.org/10.1016/J.ENVPOL.2017.12.066>
- Sharma S, Szele Z, Schilling R, Munch JC, Schloter M (2006) Influence of freeze–thaw stress on the structure and function of microbial communities and denitrifying populations in soil. *Appl Environ Microbiol* 72:2148–2154. <https://doi.org/10.1128/AEM.72.3.2148-2154.2006>
- Shi Y, Jiang Y, Wang S, Wang X, Zhu G (2020) Biogeographic distribution of comammox bacteria in diverse terrestrial habitats. *Sci Total Environ* 717:137257. <https://doi.org/10.1016/J.SCITOTENV.2020.137257>
- Singurindy O, Molodovskaya M, Richards BK, Steenhuis TS (2009) Nitrous oxide emission at low temperatures from manure-amended soils under corn (*Zea mays* L.). *Agric Ecosyst Environ* 132:74–81. <https://doi.org/10.1016/J.AGEE.2009.03.001>
- Smith J, Wagner-Riddle C, Dunfield K (2010) Season and management related changes in the diversity of nitrifying and denitrifying bacteria over winter and spring. *Appl Soil Ecol* 44:138–146. <https://doi.org/10.1016/J.APSOIL.2009.11.004>
- Song L, Zang S, Lin L, Lu B, Jiao Y, Sun C, Wang H (2022) The interaction between vegetation types and intensities of freeze–thaw cycles during the autumn freezing affected in-situ soil N₂O emissions in the permafrost peatlands of the Great Hinggan Mountains, Northeastern China. *Atmos Environ* 14:100175. <https://doi.org/10.1016/j.aeoa.2022.100175>
- Song Y, Zou Y, Wang G, Yu X (2017) Altered soil carbon and nitrogen cycles due to the freeze–thaw effect: a meta-analysis. *Soil Biol Biochem* 109:35–49. <https://doi.org/10.1016/j.soilbio.2017.01.020>
- Soosaar K, Mander Ü, Maddison M, Kanal A, Kull A, Löhmus K, Truu J, Augustin J (2011) Dynamics of gaseous nitrogen and carbon fluxes in riparian alder forests. *Ecol Eng* 37:40–53. <https://doi.org/10.1016/J.ECOLENG.2010.07.025>
- Teepe R, Brumme R, Beese F (2001) Nitrous oxide emissions from soil during freezing and thawing periods. *Soil Biol Biochem* 33:1269–1275. [https://doi.org/10.1016/S0038-0717\(01\)00084-0](https://doi.org/10.1016/S0038-0717(01)00084-0)
- Teepe R, Vor A, Beese F, Ludwig B (2004) Emissions of N₂O from soils during cycles of freezing and thawing and the effects of soil water, texture and duration of freezing. *Eur J Soil Sci* 55:357–365. <https://doi.org/10.1111/J.1365-2389.2004.00602.X>
- Thomson AJ, Giannopoulos G, Pretty J, Baggs EM, Richardson DJ (2012) Biological sources and sinks of nitrous oxide and strategies to mitigate emissions. *Philos Trans R Soc Lond B Biol Sci* 367:1157–1168. <https://doi.org/10.1098/RSTB.2011.0415>
- Viru B, Veber G, Jaagus J, Kull A, Maddison M, Muhel M, Espenberg M, Teemusk A, Mander Ü (2020) Wintertime greenhouse gas fluxes in hemiboreal drained peatlands. *Atmosphere* 11:731. <https://doi.org/10.3390/ATMOS11070731>
- Vitt DH (2006) Functional characteristics and indicators of boreal peatlands. In: *Boreal Peatland Ecosystems*, pp 9–24. https://doi.org/10.1007/978-3-540-31913-9_2
- Wagner-Riddle C, Congreves KA, Abalos D, Berg AA, Brown SE, Ambadan JT, Gao X, Tenuta M (2017) Globally important nitrous oxide emissions from croplands induced by freeze–thaw cycles. *Nat Geosci* 10:279–283. <https://doi.org/10.1038/ngeo2907>
- Wagner-Riddle C, Hu QC, Bochove E van, Jayasundara S (2008) Linking nitrous oxide flux during spring thaw to nitrate denitrification in the soil profile. *Soil Sci Soc Am J* 72:908–916. <https://doi.org/10.2136/SSSAJ2007.0353>
- Wagner-Riddle C, Rapai J, Warland J, Furon A (2011) Nitrous oxide fluxes related to soil freeze and thaw periods identified using heat pulse probes. *Can J Soil Sci* 90:409–418. <https://doi.org/10.4141/CJSS09016>
- Wang J, Song C, Miao Y, Meng H (2013) Greenhouse gas emissions from southward transplanted wetlands during freezing–thawing periods in Northeast China. *Wetlands* 33:1075–1081. <https://doi.org/10.1007/S13157-013-0463-4>
- Wang L, Sun X, Cai Y, Xie H, Zhang X (2008) Relationships of soil physical and microbial properties with nitrous oxide emission affected by freeze–thaw event. *Front Agric China* 2:290–295. <https://doi.org/10.1007/s11703-008-0058-7>
- Wang L, Xu H, Liu C, Yang M, Zhong J, Wang W, Li Z, Li K (2022) Stronger link of nosZI than nosZII to the higher total N₂O consumption in anoxic paddy surface soils. *Geoderma* 425:116035. <https://doi.org/10.1016/J.GEODERMA.2022.116035>
- van der Weerden TJ, Kelliher FM, De Klein CA (2012) Influence of pore size distribution and soil water content on nitrous oxide emissions. *Soil Res* 50:125–135. <https://doi.org/10.1071/SR11112>
- Wei Z, Shan J, Well R, Yan X, Senbayram M (2022) Land use conversion and soil moisture affect the magnitude and pattern of soil-borne N₂, NO, and N₂O emissions. *Geoderma* 407:115568. <https://doi.org/10.1016/J.GEODERMA.2021.115568>
- Wu X, Bruggemann N, Gasche R, Shen Z, Wolf B, Butterbach-Bahl K (2010) Environmental controls over soil–atmosphere exchange of N₂O, NO, and CO₂ in a temperate Norway spruce forest. *Glob Biogeochem Cycles* 24:2012. <https://doi.org/10.1029/2009GB003616>
- Wu X, Chen Z, Kiese R, Fu J, Gschwendter S, Schloter M, Liu C, Butterbach-Bahl K, Wolf B, Dannenmann M (2020a) Dinitrogen (N₂) pulse emissions during freeze–thaw cycles from montane grassland soil. *Biol Fertil Soils* 56:959–972. <https://doi.org/10.1007/S00374-020-01476-7>

- Wu X, Li T, Wang D, Wang F, Fu B, Liu G, Lv Y (2020b) Soil properties mediate the freeze-thaw-related soil N₂O and CO₂ emissions from temperate grasslands. *Catena* 195:104797. <https://doi.org/10.1016/J.CATENA.2020.104797>
- Yao Z, Wu X, Wolf B, Dannenmann M, Butterbach-Bahl K, Brüggemann N, Chen W, Zheng X (2010) Soil-atmosphere exchange potential of NO and N₂O in different land use types of Inner Mongolia as affected by soil temperature, soil moisture, freeze-thaw, and drying-wetting events. *J Geophys Res Atmos* 115:G01013. <https://doi.org/10.1029/2009JG001088>
- Yin M, Gao X, Tenuta M, Gui D, Zeng F (2019) Presence of spring-thaw N₂O emissions are not linked to functional gene abundance in a drip-fertigated cropped soil in arid northwestern China. *Sci Total Environ* 695:133670. <https://doi.org/10.1016/J.SCITOTENV.2019.133670>
- Zhang B, Penton CR, Yu Z, Xue C, Chen Q, Chen Z, Yan C, Zhang Q, Zhao M, Quensen JF, Tiedje JM (2021) A new primer set for Clade I nosZ that recovers genes from a broader range of taxa. *Biol Fertil Soils* 57:523–531. <https://doi.org/10.1007/s00374-021-01544-6>

Publisher's note Springer Nature remains neutral with regard to jurisdictional claims in published maps and institutional affiliations.

Springer Nature or its licensor (e.g. a society or other partner) holds exclusive rights to this article under a publishing agreement with the author(s) or other rightsholder(s); author self-archiving of the accepted manuscript version of this article is solely governed by the terms of such publishing agreement and applicable law.